International Journal of Thermophysics, Vol. 26, No. 4, July 2005 (© 2005)
DOI: 10.1007/s10765-005-6710-z

Electrochemical Determination of Oxidic Melt Diffusion Coefficients[1]

K. Frolov,[2,3] C. Journeau,[2,4] P. Piluso,[2] and M. Duclot[5]

The chemical diffusion coefficient of electroactive species such as Fe^{3+} and Ce^{4+} in silicate melts have been measured using an electrochemical technique: square wave voltametry. The experiments are conducted in an induction furnace in which three electrodes (made of platinum or iridium) are inserted in the crucible containing the melt. The technique has been improved to reduce the uncertainties due to the presence of a meniscus on the electrodes. Experimental results have been obtained at temperatures up to 1560 °C. The technique has proven its ability to analyze melts containing several electroactive species. These experimental results are compared to data from the literature.

KEY WORDS: chemical diffusion; high-temperature electrochemistry; silicate melts; square wave voltametry.

1. INTRODUCTION

Chemical diffusion is a complex phenomenon in oxidic liquids, especially in silicate melts [1], which is of major relevance for geophysical as well as industrial processes. For instance, it governs the element fractionation between minerals and melts [2] and the rates of crystal growth as well as the diffusion of dopants in glasses and the corrosion processes of metals

[1] Paper presented at the Seventh International Workshop on Subsecond Thermophysics, October 6–8, 2004, Orléans, France.

[2] CEA Cadarache, DEN/DTN/STRI, Severe Accident Mastering Experimental Laboratory, Building 708, 13108 St Paul lez Durance Cedex, France.
[3] Current address: Kurchatov Institute, Nuclear Safety Institute, Kurchatov Sq., Moscow 123182, Russia.
[4] To whom correspondence should be addressed. E-mail: christophe.journeau@cea.fr
[5] LEPMI–ENSEEG (UMR 5631 CNRS, INPG, UJF) 1130 rue de la Piscine, BP 5, 38402 Saint Martin d′Hères, France.

0195-928X/05/0700-1181/0 © 2005 Springer Science+Business Media, Inc.

in contact with molten glasses [3]. Chemical diffusion is considered to be one of the main processes controlling the solidification of multicomponent oxide melts that would occur in the hypothetical case of a nuclear reactor severe accident [4,5]. For the late phase of a severe accident, which would follow the corium–concrete interaction, the multicomponent ex-vessel corium melt is considered as one containing a certain fraction of silica, between 5 and 30 mol%, according to current estimations.

Numerous experimental techniques have been proposed to measure chemical diffusivity: radiochemical tracers (e.g., Ref. [6]), spectroscopy (see e.g. numerous applications in [7]), nuclear magnetic resonance [8], as well as electrochemical techniques (e.g., Ref. [9]) such as chronoamperometry and voltametry.

High temperatures (1300–2200°C) require minimization of the experiment duration, and the use of low thermal diffusivity oxides precludes the possibility of efficient quenching. Square wave voltametry [10,11] has been selected for our tests due to its ability to take a rapid measurement and to measure simultaneously the auto-diffusion coefficient for several constituents.

In this paper, we will first present the experimental setup which has been used in the VITI facility, then the square wave voltametry will be presented, as well as some improved features. Finally, experimental results will be presented and discussed.

2. EXPERIMENTAL SETUP

The VITI facility [12], initially used for viscosity measurements, has been modified in the view of electrochemical measurements (Fig. 1). Oxides loaded in a ceramic crucible (3) can be molten with an induction furnace made of a coil (6) and a graphite susceptor (8). The measuring electrodes (1) are dipped in the melt using the micrometric table (5). The melt temperature is measured with a pyrometer (4) and a tungsten–rhenium thermocouple (2). The whole setup is installed inside the VITI vessel (11).

Figure 2 presents the measurement probes. It consists mainly of a set of three electrodes (in platinum or iridium, depending on the temperature range) which are connected to a DEA 332 potentiostat. The potentiostat imposes the working electrode potential which is varied relative to the reference electrode. It is also used to measure the voltage and intensity response of the circuit between the working and auxiliary electrodes. An impedance meter is used to determine the melt-free surface position. Figure 3 shows a global view of this setup.

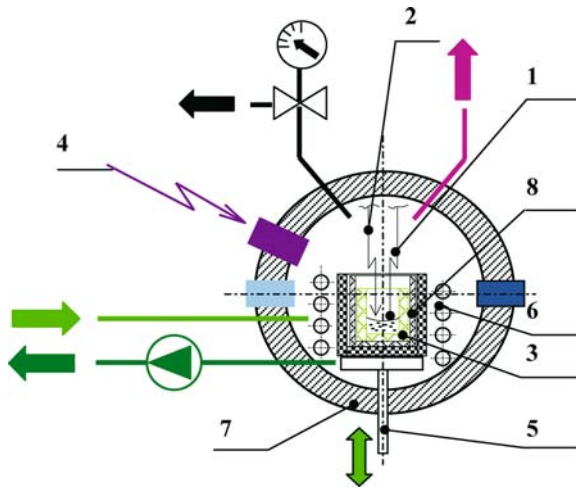

Fig. 1. VITI facility with the electrochemical setup.

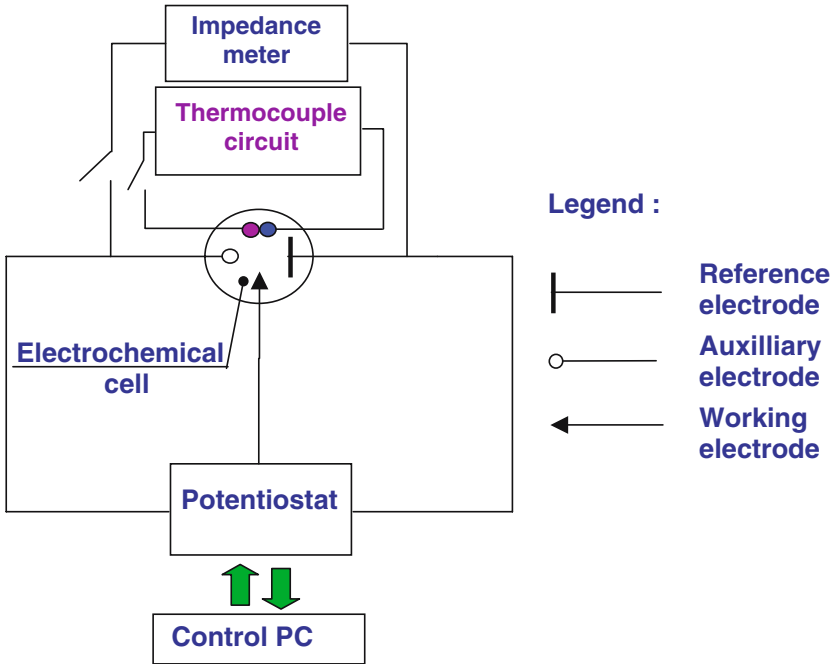

Fig. 2. Electrical scheme of the measurement probes.

Fig. 3. Photograph of the measurement setup.

3. SQUAREWAVE DIFFERENTIAL VOLTAMETRY

For ideal mixtures, the fluxes of the electroactive species under an imposed potential difference verify the Nernst–Planck equation:

$$J_i = -D_i \frac{dC_i(x)}{dx} - \frac{Z_i F}{RT} D_i C_i \frac{d\phi(x)}{dx} + C_i v(x), \tag{1}$$

where J_i is the flux of the electroactive species ($\text{mol} \cdot \text{m}^{-2} \cdot \text{s}^{-1}$), C_i is the concentration of the electroactive species ($\text{mol} \cdot \text{m}^{-3}$), D_i is the diffusion coefficient of the electroactive species ($\text{m}^2 \cdot \text{s}^{-1}$), Z_i is the charge of the electroactive species, F is Faraday's constant ($F = 96485.3\, C \cdot \text{mol}^{-1}$), φ is the electrostatic potential (V), R is the universal gas constant ($\text{R} = 8.315\, J \cdot \text{K}^{-1} \cdot \text{mol}^{-1}$), T is the melt temperature (K), v is the characteristic velocity of the melt ($\text{m} \cdot \text{s}^{-1}$), and x is the coordinate (m). A more rigorous approach for multicomponent systems can by found in Ref. 14.

Neglecting effects of convection for a subsecond period following a voltage step, Eq. (1) implies that the flux of an electroactive species will be controlled by the electrical field and the electroactive species concentration gradient in the boundary layer near the electrode. Voltametric techniques are designed to create this gradient. In square wave voltametry, the following series of staircase voltages are applied between the electrodes, as shown in Fig. 4:

$$E_m = E_i + \left[\text{Int}\left(\frac{m+1}{2} \right) + 1 \right] \Delta E_S - (-1)^m \Delta E_p. \tag{2}$$

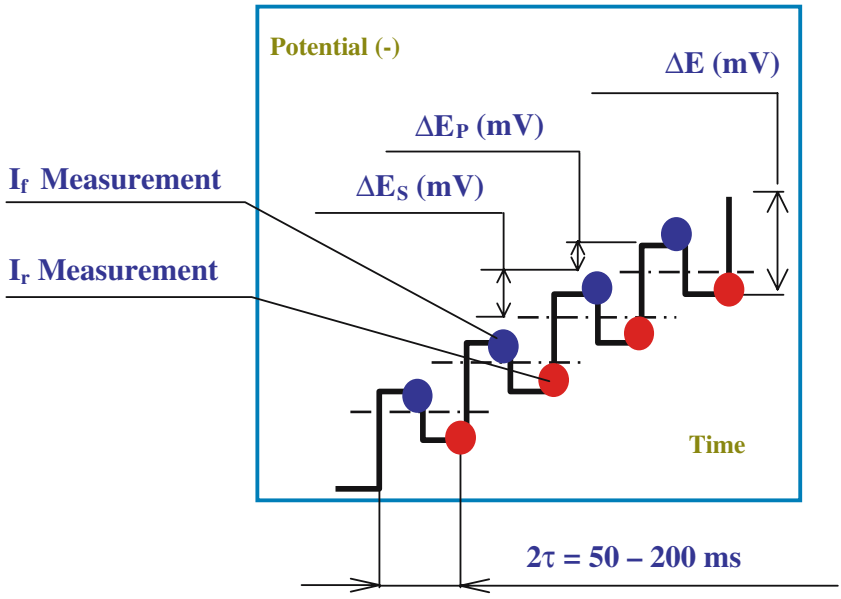

Fig. 4. Voltage Signal used for the square wave voltametry.

The initial potential E_i is chosen such that, on the one side, none of the electroactive species of interest in the melt can be reduced and, on the other side, no gaseous oxygen is formed at the anode, while the final potential is such that all these electroactive species are reduced without reaching a deposit of silicium or silicide on the cathode. For the silicate melts of interest (where the $Fe^{3+} + e^- \rightarrow Fe^{2+}$ and $Ce^{4+} + e^- \rightarrow Ce^{3+}$ RedOx couples were studied) a potential range between −750 mV and +750 mV relative to a platinum reference electrode was considered. The time step is chosen (in the 50–200 ms range) in order to allow for Faradic discharge while being shorter than the characteristic time for the onset of convection.

Figure 5 presents the current generated by a square voltage signal. The current is measured at the end of each half-period (corresponding to the blue and red points in Figs. 4 and 5). The difference δI between the forward and reverse currents (i.e., the currents measured at the ends of the upward and downward steps, the times marked with the blue and red points on Fig. 4) is plotted against the step mean potential as in Fig. 6.

For potentials far from the standard potential of the RedOx couple, the current varies slowly with the potential, and the net current δI tends to zero. On the opposite, the difference will be important if an electroactive

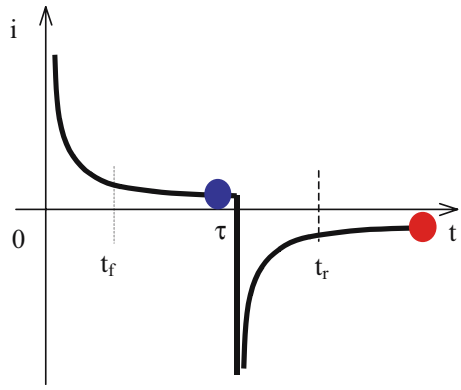

Fig. 5. Response to a forward step followed by a reverse step.

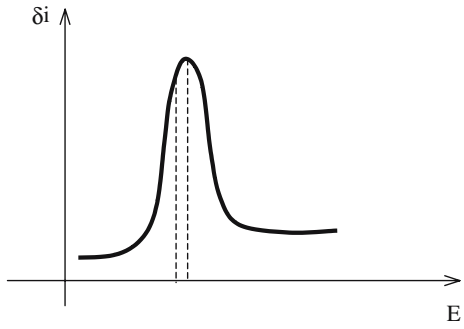

Fig. 6. Net current measured in response of the voltage steps from Fig. 4.

species is totally reduced in the first half period and totally oxidized in the second half period. Rüssel [13] has shown that the peak value I_P of the net current is expressed by

$$I_p = A_W C_0 D^{0.5} \frac{an^2 F^2 \Delta E}{RT\tau^{0.5}}, \tag{3}$$

where ΔE is the pulse characteristic voltage increase as defined in Eq. (2), a is a constant, here a = 0.31, A_W is the contact area between the working electrode and the melt (m^2), D is the chemical diffusion coefficient of the electroactive species ($m^2 \cdot s^{-1}$), n is the number of electrons exchanged for the half RedOx reaction occurring on the working electrode, and τ is the pulse halfwidth (s).

The diffusion coefficient is thus proportional to the square of the net current. Uncertainty analysis shows that the major source of error involves

the determination of the contact area, mainly due to the presence of a meniscus of unknown shape at the melt free surface. Measurement precision has been increased by making measurements at two successive depths. For a cylindrical electrode of diameter d, the net current increase ΔI_p due to a variation of depth Δl is given by

$$\frac{\Delta I_p}{\Delta l} = \pi d C_0 D^{0.5} \frac{an^2 F^2 \Delta E}{RT\tau^{0.5}}. \tag{4}$$

With this improved technique, the relative uncertainty has been estimated for our experimental cases [14] to be of the order of 20%. Thus, it is not necessary to measure the absolute immersion depth.

One of the authors [14] has rigorously proven that the diffusion coefficient which is used in Eqs. (3) and (4) is the effective binary diffusion coefficient which reduces to the self-diffusion coefficient when the concentration in the electroactive species tends to zero.

4. EXPERIMENTAL RESULTS

A first series of experiments aimed at validating the experimental setup with Fe^{3+}/Fe^{2+} tracers in a 10 mol%CaO – 16 mol% Na_2O – 74 mol% SiO_2 melt which has been previously studied by Rüssel [13]. These experiments were conducted under helium atmosphere. The distance between the electrodes varied around 5–10 mm throughout this experimental program. Their characteristics are listed in Table I.

Figure 7 presents a typical net current measurement. The peak was obtained for this series in the [−530, −430 mV] range, where the standard potential of the Fe^{3+}/Fe^{2+} RedOx couple lies at the temperatures of interest. The variations are attributed to the variations of temperature between tests. Actually, in order to avoid electromagnetic interferences between the induction heating and the electrochemical measurements, the heating had to be turned off during the measurement.

Figure 8 presents a typical temperature measurement with a cooling rate around $15\,K\cdot s^{-1}$ for a signal sweep rate of $200\,mV\cdot s^{-1}$.

From successive measurements at two depths 1 mm apart, it has been possible to determine, using Eq. (4), the diffusion coefficient. These values (Table II) are close (logarithmic error < 0.6) to those that were measured on the same melt by Rüssel [13], of the same amplitude than the difference between Rüssel's data [13] and those of Takahashi and Miura [15] which were obtained with the linear sweep voltametry technique on a very close composition (12% CaO, 16% Na_2O, 72% SiO_2). Anyhow, it

Table I. Characteristics of the Tests with 10 mol% CaO –16 mol% Na_2O–74 mol% SiO_2

Potential windows, $E(10^{-3}$ V)	Pulse amplitude, $\Delta E(10^{-3}$ V)	Pulse period, $\tau(10^{-3}$ s)	Temperature (°C)	Peak net current $(10^{-3}$ A)
−800 to 800	100	50–400	1350–1430	2–15

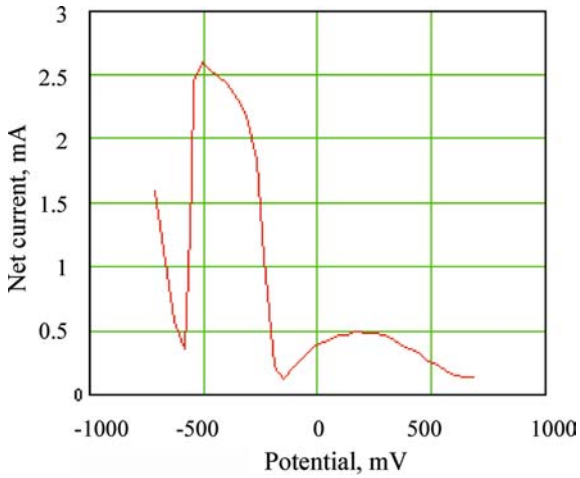

Fig. 7. SWV measurement for 100 ms pulses in 10 mol% CaO – 16 mol% Na_2O – 74 mol% SiO_2.

must be stressed that in most of the applications, it is the order of magnitude of the diffusion coefficient rather than its precise value that is needed [14].

In a second series of experiment, a mixture containing two electroactive species (Fe^{3+}, Ce^{4+}) has been studied. Its composition was: 10 mol% CaO, 11.9 mol% Na_2O, 76.8 mol% SiO_2, 0.7 mol% Fe_3O_4, and 0.6 mol% CeO_2. Four measurements have been obtained at different depths. Two distinctive peaks have been observed on Fig. 9 and have been attributed to the $Fe^{3+} + e^- \rightarrow Fe^{2+}$ and $Ce^{4+} + e^- \rightarrow Ce^{3+}$ RedOx couples. The shift in the peak potential is due to the fact that the melt temperature varied with the immersion depth, since lowering the electrodes contributes to the thermal insulation of the crucible. The experimental data have been reported in Table III. The measured diffusion coefficient values are within 0.3 logarithmic units of the data from Rüssel [13] for Fe^{3+} and Takahashi and Miura [15] for Ce^{4+} (in these measurement reports only

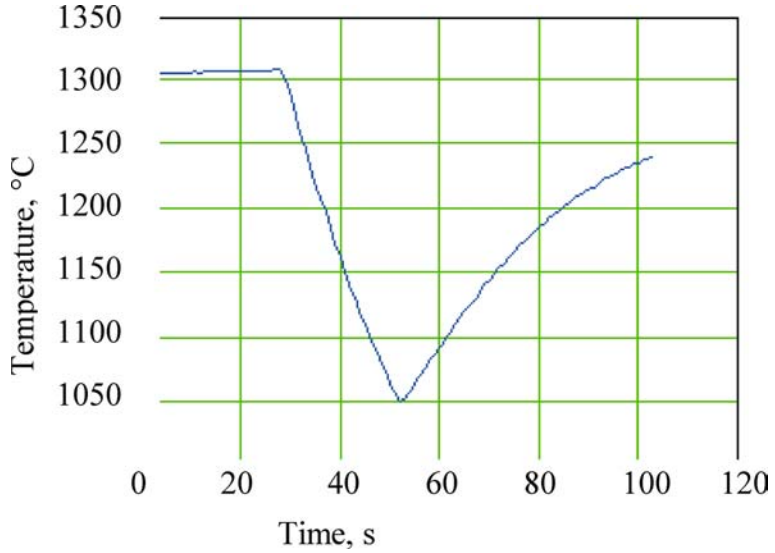

Fig. 8. Temperature evolution just above the melt (potential swept at $200\,mV \cdot s^{-1}$).

Table II. Diffusion Coefficient for 10 mol% CaO – 16 mol% Na_2O – 74 mol% SiO_2

Temperature, T (°C)	Depthincrement, Δl (mm)	Peak current increment, ΔI (mA)	Measured diffusion coefficient ($m^2 \cdot s^{-1}$) (this work)	Diffusion coefficient ($m^2 \cdot s^{-1}$) [13]
1400	1	1.6	$10^{-9.23}$	$10^{-9.64}$
1300	3.2	3.36	$10^{-10.6}$	$10^{-10.0}$

one of the tracers was present). Temperature variations are lower than the uncertainties.

In a third series of tests, a 34.4%$_{mol}$ CaO – 64.5% SiO_2 – 1.1% Fe_3O_4 melt has been successfully measured at an higher temperature (around 1547 °C) using an iridium reference electrode. The diffusion coefficient has been estimated to be of the order of 10^{-10} in the 1557–1561 °C range and of 10^{-11} in the 1534–1547 °C range.

5. CONCLUSIONS

An experimental setup has been installed in the VITI facility in order to determine diffusion coefficients in silicate melts. It is based on the

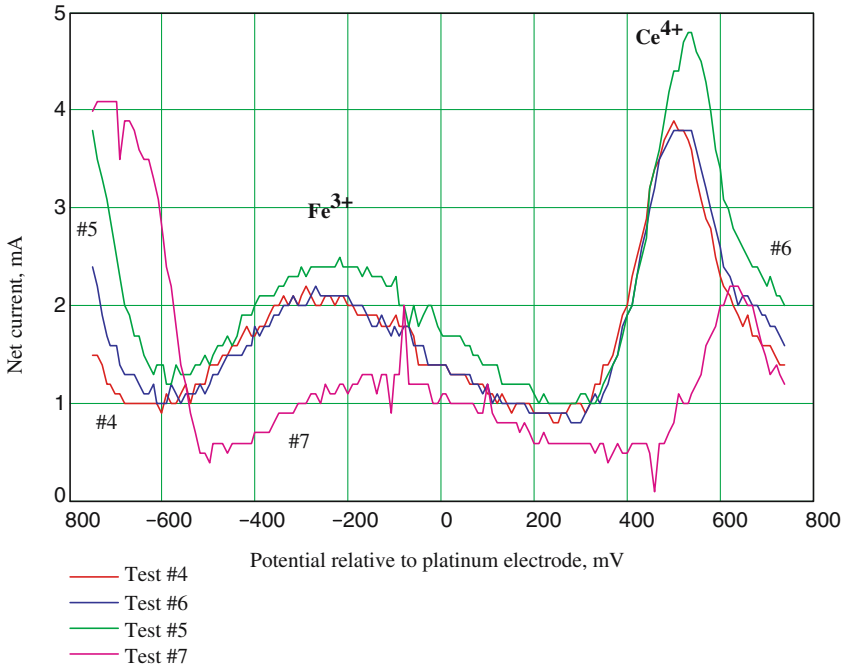

Fig. 9. SWV plots for the melt containing Fe^{3+} and Ce^{4+}.

square wave voltametry which has been improved to reduce the uncertainty on the electrode area due to the presence of a meniscus.

This technique has been validated at temperatures up to 1560 °C and has shown its ability to analyze melts containing several electroactive species, provided their RedOx standard potentials are far enough apart. It is planned to use this technique to estimate diffusion coefficient

Table III. Characterization of the Tests with Fe^{3+} and Ce^{4+}

Test #	Depth (relative to test #4) Δl (mm)	Fe^{3+} peak potential (10^{-3} V)	T (°C)	Fe^{3+} Peak net current increment, ΔI_p (10^{-3} A) (log (D[$m^2 \cdot s^{-1}$])	Measured Fe^{3+} diffusion coefficient	Fe^{3+} diffusion coefficient according to Rüssel [13]
4	–	−291	1370	–	–	−9.72
5	0.5	−271	1379	0.1	−10.58	−9.7
6	1.0	−221	1384	0.4	−9.98	−9.75
7	−1.0	−160	1355	−0.8	−9.39	−9.78

Table IV. continued

	Ce^{4+} peak potential (10^{-3} V)	T(°C)	Ce^{4+} Peak net current increment, ΔI_p(10^{-3} A)	Measured CE^{4+} diffusion coefficient log (D[$m^2 \cdot s^{-1}$])	Ce^{4+} Diffusion coefficient according to Takahashi and Miura [15]
4	499	1310.5	–	–	
5	519	1317.2	0.2	−9.88	−8.87
6	539	1327.9	1.0	−9.08	−8.79
7	629	1296.5	−1.6	−8.69	−9.03

with uranium-containing melts in order to model the interaction between molten core and concrete during an hypothetical nuclear reactor severe accident.

ACKNOWLEDGMENTS

This work was performed thanks to a Ph.D. grant from CEA's International Relations Divisions. The work and efforts of the VITI experimental team are greatly acknowledged.

REFERENCES

1. S. Chakraborthy, in *Structures, Dynamics and Properties of Silicate Melts*, J. F. Stebbins, P. F. McMillans, and D. B. Dingwell, eds. (Mineralogical Soc. Am., Washington, D.C., 1995), pp. 411–503.
2. A. Prinzhofer and C. J. Allègre, *Earth Planet. Sci. Lett.* **74**:251 (1985).
3. C. Rüssel and A. Kämpfer, *Glastech. Ber. Glass* **71**:6 (1998).
4. J. M. Seiler and K. Froment, *Multiphase Sci. Technol.* **12**:117 (2000).
5. C. Journeau, C. Jégou, J. Monerris, P. Piluso, K. Frolov, Yu. B. Petrov, and R. Rybka, in *Proc. 10th Int. Top. Mtg. Nucl. React. Thermalhydraulics* (NURETH-10, Seoul, 2003), Paper G00301.
6. P. Kubiček and T. Pepřica, *Int. Met. Rev.* **28**:131 (1983).
7. H. J. V. Tyrrell and K. R. Harris, *Diffusion in Liquids* (Butterworths, London, 1984).
8. J. F. Stebbins, in *Structures, Dynamics and Properties of Silicate Melts*, J. F. Stebbins, P. F. McMillans, and D. B. Dingwell, eds. (Mineralogical Soc. Am., Washington, D.C., 1995), pp. 191–246.
9. A. J. Bard and L. R. Faulkner, *Electrochemical Methods. Fundamentals and Applications* (Wiley, New York, 2001).
10. J. G. Osteryoung and R. A. Osteryoung, *Anal. Chem.* **57**:101 (1985).
11. C. Montel, C. Rüssel, and E. Freude, *Glastech. Ber. – Glass* **61**:59 (1988).
12. P. Piluso, J. Monerris, C. Journeau, and G. Cognet, *Int. J. Thermophys.* **23**:1229 (2002).
13. C. Rüssel, *J. Non-Crystal. Solids* **134**:169 (1991).

14. K. Frolov, *Diffusion Chimique à l'état liquide dans des bains silicates. Applications aux accidents graves de réacteurs nucléaires* (Ph. D. Thesis, Université Joseph Fourier, Grenoble, 2004).
15. K. Takahashi and Y. Miura, *J. Non-Crystal. Solids* **80**:11 (1986).